Discontinuous transitions in double-exchange materials

J. L. Alonso,[1] L. A. Fernández,[2] F. Guinea,[3] V. Laliena,[1] and V. Martín-Mayor[4]
[1]*Departamento de Física Teórica, Facultad de Ciencias, Universidad de Zaragoza, 50009 Zaragoza, Spain*
[2]*Departamento de Física Teórica, Facultad de CC. Físicas, Universidad Complutense de Madrid, 28040 Madrid, Spain*
[3]*Instituto de Ciencia de Materiales (CSIC), Cantoblanco, 28049 Madrid, Spain*
[4]*Dipartimento di Fisica, Università di Roma ''La Sapienza,'' Piazzale Aldo Moro 2, 00185 Roma and INFN sezione di Roma, Italy*
(Received 30 June 2000; published 22 January 2001)

It is shown that the double-exchange Hamiltonian, with weak antiferromagnetic interactions, has a rich variety of first-order transitions between phases with different electronic densities and/or magnetizations. The paramagnetic-ferromagnetic transition moves towards lower temperatures, and becomes discontinuous as the relative strength of the double-exchange mechanism and antiferromagnetic coupling is changed. This trend is consistent with the observed differences between compounds with the same nominal doping, such as $La_{2/3}Sr_{1/3}MnO_3$ and $La_{2/3}Ca_{1/3}MnO_3$. Our results suggest that, in the low doping regime, a simple magnetic mechanism suffices to explain the main features of the phase diagram.

DOI: 10.1103/PhysRevB.63.064416 PACS number(s): 75.10.−b, 75.30.Et

I. INTRODUCTION

Doped manganites show many unusual features, the most striking being the colossal magnetoresistance (CMR) in the ferromagnetic (FM) phase.[1–3] In addition, the manganites have a rich phase diagram as function of band filling, temperature, and chemical composition. The broad features of these phase diagrams can be understood in terms of the double-exchange model (DEM),[4,5] although Jahn-Teller deformations[6] and orbital degeneracy may also play a role.[7] A remarkable property of these compounds is the existence of inhomogeneities in the spin and charge distributions in a large range of dopings, compositions, and temperatures.[8–10] At band fillings where CMR effects are present, $x \sim 0.2–0.5$, these compounds can be broadly classified into those with a high Curie temperature and a metallic paramagnetic phase, and those with lower Curie temperatures and an insulating magnetic phase.[11–13]

The DEM is a simplification of the FM Kondo lattice, where the FM coupling between core spins and conduction electrons is due to Hund's rule. When this coupling is larger than the width of the conduction band, the model can be reduced to the double-exchange model with weak interatomic antiferromagnetic (AFM) interactions (see below). Early investigations[14] showed a rich phase diagram, with AFM, canted and FM phases, depending on doping and the strength of the AFM couplings. More recent studies have shown that the competition between the double-exchange and the AFM couplings leads to phase separation into AFM and FM regions, suppressing the existence of canted phases.[15–17,19] In addition, the double-exchange mechanism alone induces a change in the order of the FM transition, which becomes of first order, and leads to phase separation, at low dopings.[20] Note, however, that a detailed study of the nature of the transition at finite temperatures is still lacking, despite its obvious relevance to the experiments.

The purpose of this work is to investigate systematically the phase diagram of the DEM with weak AFM interactions. Our work applies to compounds of the type $R_{1-x}A_xMnO_3$, where R is a lanthanide, and A is a divalent cation (like Ca or Sr), in the range $0.2 \leqslant x \leqslant 0.5$, which includes the doping levels where CMR has been observed, and where the double-exchange model is appropriate (see below). We will focus on the doping dependence, and also on the observed differences between compounds with the same nominal doping, such as $La_{1-x}Ca_xMnO_3$ and $La_{1-x}Sr_xMnO_3$, which exhibit, however, different values of the Curie temperature, and where even the order of the transition is different (continuous in the case of $La_{1-x}Sr_xMnO_3$ and discontinuous in the case of $La_{1-x}Ca_xMnO_3$). Our goal is to find the simplest model compatible with these observations. The importance of AFM interactions in inducing differences between manganites with the same nominal doping has already been emphasized in Refs. 21 and 22.

We find, in addition to the transitions previously discussed in the literature, a first-order transition near half filling, if the double-exchange mechanism is sufficiently reduced by the AFM interactions. This transition does not involve a significant change in electronic density, so that domain formation is not suppressed by electrostatic effects. The main features of the phase diagram obtained are consistent with the observed dependence on doping. Assuming that a change in the divalent cation modifies the balance between the AFM couplings and the double-exchange mechanism, the differences between compounds with the same nominal doping can also be understood.

The model is described in the next section, and the method of calculation is introduced in the following section. The main results are presented in Sec. IV, and the main conclusions are discussed in Sec. V.

II. MODEL

We study a cubic lattice with one orbital per site. At each site there is also a classical spin. The coupling between the conduction electron and this spin is assumed to be infinite, so that the electronic state with spin antiparallel to the core spin can be neglected. Finally, we include an AFM coupling between nearest-neighbor core spins.[18] The Hamiltonian is

$$\mathcal{H}=\sum_{ij}\ \mathcal{T}(\boldsymbol{S}_i,\boldsymbol{S}_j)c_i^{\dagger}c_j+\sum_{\langle i,j\rangle}\ \tilde{J}_{\mathrm{AF}}S^2\boldsymbol{S}_i\cdot\boldsymbol{S}_j, \tag{1}$$

where $S=3/2$ is the value of the spin of the core, Mn^{3+}, and $\boldsymbol{S}$ stands for a unit vector oriented parallel to the core spin, which we assume to be classical. In the following, we will use $J_{\mathrm{AF}}=\tilde{J}_{\mathrm{AF}}S^2$. Calculations show that the quantum nature of the core spins does not induce significant effects.[17] The function $\mathcal{T}(\boldsymbol{S}_i,\boldsymbol{S}_j)=t[\cos(\theta_i/2)\cos(\theta_j/2)+\sin(\theta_i/2)\sin(\theta_j/2)e^{i(\varphi_i-\varphi_j)}]$ stands for the overlap of two spin 1/2 spinors oriented along the directions defined by $\boldsymbol{S}_i$ and $\boldsymbol{S}_j$, whose polar and azimuthal angles are denoted by θ and φ, respectively. We study materials of composition $La_{1-x}M_xMnO_3$, where M is a divalent ion, and $x\leqslant 0.5$. In this composition range, the probability of finding two carriers in neighboring sites (two contiguous Mn^{4+} ions) is small, so that a carrier in a given ion has all the e_g orbitals in the next ions available. Then, the anisotropies associated to the differences between the two inequivalent e_g orbitals should not play a major role. On the other hand, if $x\geqslant 0.5$, we expect a significant dependence of the hopping elements on the occupancy of orbitals in the nearest ions. In this regime, the equivalence of the two e_g orbitals in a cubic lattice can be broken, leading to orbital ordering[7,23] (see, however, Ref. 24). We will show that the main features of the paramagnetic (PM)-FM phase transition, for $x\leqslant 0.5$, can be understood without including orbital ordering effects. Moreover, in this doping range, anisotropic manganites show similar features,[25–28] which suggest the existence of a common description for the transition. We will also neglect the coupling to the lattice. As mentioned below, magnetic couplings suffice to describe a number of discontinuous transitions in the regime where CMR effects are observed. These transitions modify substantially the coupling between the conduction electrons and the magnetic excitations. Thus they offer a simple explanation for the anomalous transport properties of these compounds. Couplings to additional modes, like optical or acoustical phonons,[29] and dynamical Jahn-Teller distortions[30] will enhance further the tendency towards first-order phase transitions discussed here. We consider that a detailed understanding of the role of the magnetic interactions is required before adding more complexity to the model.

III. METHOD

At finite temperatures, the thermal disorder in the orientation of the core spins induces off-diagonal disorder in the dynamics of the conduction electrons. The calculation of the partition function requires an average over core spin textures, weighted by a Boltzmann factor which depends on the energy of the conduction electrons propagating within each texture. We have simplified this calculation by replacing the distribution of spin textures by the one induced by an effective field acting on the core spins, which is optimized so as to minimize the free energy. The electronic energy includes accurately the effects of the core spin disorder on the electrons. Our calculation is a mean-field approximation to the thermal fluctuations of the core spins, retaining, however, the complexity of a system of electrons with off-diagonal disorder.[31] This approximation can be justified by noting that the conduction electrons induce long-range interactions between the core spins, that always favor a FM ground state. In general, our method is well suited for problems of electrons interacting with classical fields.

In more mathematical terms, we have used the variational formulation of the Weiss mean-field method[32] to compute the free energy of the system. We first trace out the fermion operators in Eq. (1), thus obtaining the effective Hamiltonian for the spins,

$$\mathcal{H}^{\mathrm{eff}}(\{\boldsymbol{S}\})=J_{\mathrm{AF}}\sum_{\langle i,j\rangle}\boldsymbol{S}_i\cdot\boldsymbol{S}_j-k_{\mathrm{B}}TV\int dE\,g(E;\{\boldsymbol{S}\})\times\ln[1+e^{-(E-\mu)/(k_{\mathrm{B}}T)}], \tag{2}$$

where $g(E;\{\boldsymbol{S}\})$, is the fermionic density of states and V the volume of the system. The mean-field procedure consists on comparing the system under study with a set of simpler reference models, whose Hamiltonian $\mathcal{H}_0$ depends on external parameters. We choose

$$\mathcal{H}_0=-\sum_i\ \boldsymbol{h}_i\cdot\boldsymbol{S}_i\,. \tag{3}$$

The variational method follows from the inequality

$$\mathcal{F}\leqslant\mathcal{F}_0+\langle\mathcal{H}_{\mathrm{eff}}-\mathcal{H}_0\rangle_0\,, \tag{4}$$

where $\mathcal{F}_0$ is the free energy of the system with Hamiltonian (3), and the expectation values $\langle\cdot\rangle_0$ are calculated with the Hamiltonian $\mathcal{H}_0$. The mean fields $\{\boldsymbol{h}\}$ are chosen to minimize the right-hand side of Eq. (4). The calculation of the right-hand side of Eq. (4) requires the average of the density of states [see Eq. (2)] on spin configurations straightforwardly generated according to the Boltzmann weight associated to the Hamiltonian $\mathcal{H}_0$ and temperature T. The key point is that $g(E;\{\boldsymbol{S}\})$ can be numerically calculated on very large lattices without further approximations using the method of moments[33] (complemented with a standard truncation procedure[34]). We have extracted the spin-averaged density of states on a $64\times64\times64$ lattice (for these sizes, we estimate that finite-size effects are negligible). For simplicity on the analysis, we have restricted ourselves to four families of fields: uniform, $\boldsymbol{h}_i=\boldsymbol{h}$, giving rise to FM ordered textures; $\boldsymbol{h}_i=(-1)^{z_i}\boldsymbol{h}$, originating A-AFM order, i.e., textures that are FM within planes and AFM between planes; $\boldsymbol{h}_i=(-1)^{x_i+y_i}\boldsymbol{h}$, producing C-AFM order, that is, textures that are FM within lines and AFM between lines; and staggered, $\boldsymbol{h}_i=(-1)^{x_i+y_i+z_i}\boldsymbol{h}$, which originate G-AFM order, i.e., completely AFM textures. We have chosen fields of these kind since they produce the expected kinds of order, although this is not a limitation of the method. Once the spin-averaged density of states is obtained, it is straightforward to obtain the values of the mean-field that minimize the right-hand side of Eq. (4), and the corresponding value of the density of fermions. Expressing the right-hand side of Eq. (4) as a function of the magnetization (or staggered magnetizations), we obtain the Landau's expansion of the free energy on the order parameter.

It is finally worth mentioning when our calculation and the dynamical mean-field approximation (DMFA) (Refs. 19,35) are expected to yield the same results. It is clear that the key point is the calculation of the density of states. For this problem of classical variables, the dynamical mean field is known to yield the same density of states as the CPA approximation.[36] Under the hypothesis of spatially uncorrelated fluctuations of the spins, which holds in any mean-field approximation, the CPA becomes exact on the Bethe lattice with large coordination number. However, one cannot conclude that with our calculation we would get the same results on the Bethe lattice, since one has still to specify the probability distribution for the spins to be used in the CPA calculation of the average density of states. In Refs. 35 and 19 the calculation is done by identifying an effective Heisenberg-like mean field, which becomes exact when the magnetization is very small. Then, the distribution of spin orientations is equivalent to the one generated by an effective magnetic field. In this limit, our *Ansätz* should reproduce the calculations reported in Refs. 35 and 19 when implemented in a Bethe lattice.

In order to study first order transitions, one must consider solutions at finite magnetizations. Then, the optimal Boltzmann weights need not coincide with the effective-field *Ansätz* made here. Detailed DMFA calculations for the double-exchange model,[37,38] however, show that the differences between the optimal DMFA distribution and that obtained with an effective field are small throughout the entire range of magnetizations. Thus the scheme used in this work includes the same physical processes as the DMFA, but it is also able to describe effects related to the topology of the three-dimensional lattice, like those associated to the Berry phase, which arises from the existence of closed loops. Furthermore, the present scheme allows us to study the relative stability of phases, like the *A* and *C* antiferromagnetic phases described below, which can only be defined in a cubic lattice.

IV. RESULTS

The model, Eq. (1), contains two dimensionless parameters: the doping x and the ratio J_{AF}/t. The range of values of x is $0 \leqslant x \leqslant 1$, and the Hamiltonian has electron-hole symmetry around $x=0.5$. The zero-temperature phase diagram, shown in Fig. 1, is calculated minimizing the effective Hamiltonian at fixed chemical potential and zero temperature [we take the limit of zero temperature in Eq. (2) obtaining the grand-canonical Hamiltonian], within the four mean-field *Ansätze* previously defined. At zero J_{AF}/t, only the ferromagnetic phase is found, and the system is stable at all compositions. When J_{AF}/t is finite, there is a value of the chemical potential for which the empty system with a perfect *G*-type AFM spin ordering has the same *grand-canonical* energy that a system with a perfect FM spin ordering and a finite value of x. At this value of the chemical potential the system is unstable against phase separation,[20] as shown in Fig. 1. Notice that the phase-separation region can never reach $x=0.5$, due to the hole-particle symmetry. For larger values of J_{AF} a small region of *A*-type AFM is found for x

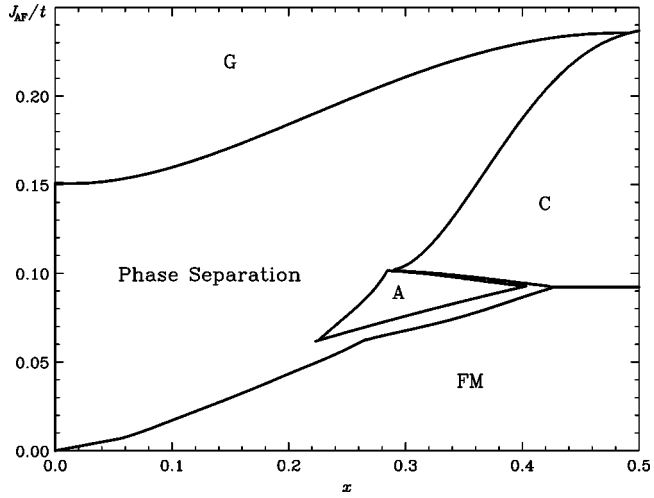

FIG. 1. Calculated phase diagram at $T=0$. The *A*-AFM phase has ferromagnetic alignment within planes, and antiferromagnetic alignment between parallel planes. The *C*-AFM phase has ferromagnetic alignment along chains, and antiferromagnetic alignment between neighboring chains.

~ 0.25, and a much larger region of *C*-type AFM for x close to half filling. Finally, a *G*-type AFM region is eventually reached by further increasing J_{AF}/t. However, this is not a saturated antiferromagnetic phase since the mean field that minimizes the grand-canonical energy has a finite $\boldsymbol{h}/T$ when T tends to zero[39] (notice that one cannot have a continuously varying value of x in a perfect AFM configuration).

Let us now discuss the phase diagrams at nonzero temperatures for the different values of J_{AF}/t shown in Fig. 2. For $J_{\mathrm{AF}}=0$, we obtain a maximum transition temperature of $T=400$ K for a width of the conduction band $W=12t \approx 2$ eV, which is consistent with a density of states of $\rho(E_{\mathrm{F}})=0.85\ \mathrm{eV}^{-1}$ calculated in Ref. 41 for $La_{1/3}Ca_{2/3}MnO_3$ (see also Ref. 42). Note that the bandwidth

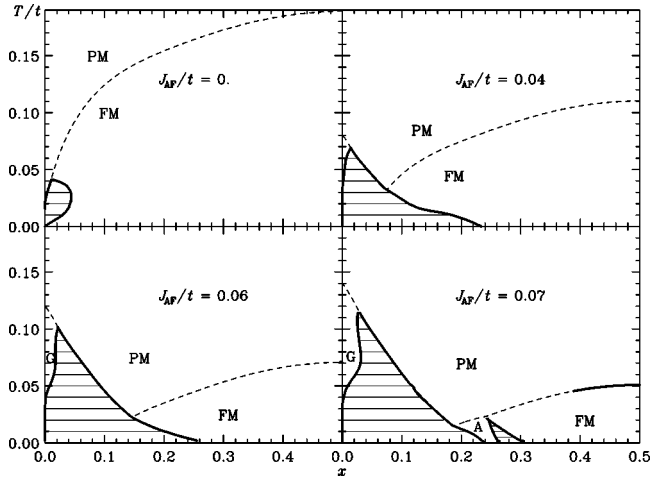

FIG. 2. Transition temperatures as function of electronic density and strength of the AFM couplings. The dashed lines correspond to continuous transitions. Solid thick lines are drawn for first-order transitions, and the stripes correspond to phase coexistence regions. The onset of first order transitions at $x \sim 0.5$ is $J_{\mathrm{AF}}/t \approx 0.06$.

calculated in this way is probably an overestimate, as it does not include renormalization effects due to lattice vibrations.[43] There is some controversy regarding the value of J_{AF}. The reported value of J_{AF} for the undoped compound $LaMnO_3$ is $\tilde{J}_{AF} \approx 0.58$ meV, so that $J_{AF} \approx 0.005t$,[44] although calculations give higher values.[45] If the intraatomic Hund's coupling between the e_g electrons and the core spin is not too large, there is an additional contribution of order $J_{AF} \sim t^2/U_{ex}$, where U_{ex} is the level splitting induced by the intra-atomic Hund's coupling [note that $U_{ex} \approx 1-2$ eV(see Ref. 3)]. This term is due to virtual hoppings of an electron in the e_g orbital to a vacant e_g orbital in a neighboring Mn ion with spin antiparallel to the core. These orbitals lie at an energy $\sim J_H$ above the energy of the orbital with spin parallel to the core. These processes, which contribute to the delocalization of the e_g electrons, are suppressed by a factor $\sim t/U_{ex}$, lowering the electronic kinetic energy by an amount $\sim t^2/U_{ex}$. These processes are only possible if the core spins of the neighboring Mn ions are antiparallel, leading to an effective antiferromagnetic coupling. Thus $J_{AF} \sim 0.01t-0.08t$, although higher values have been suggested.[7] The previous discussion does not take into account the effect of the Mn-O-Mn bond angle on the direct superexchange interaction between the core spins, which is also altered upon doping.[11] Finally, the ratio J_{AF}/t depends on the choice of divalent cation.[22] In the following, we will use J_{AF} as an adjustable parameter, which can be modified by doping and the choice of divalent cation.

Our results show four types of first-order transitions:

(i) In pure DEM ($J_{AF}=0$) the magnetic transition becomes discontinuous at sufficiently low densities, in agreement with the analysis presented in Ref. 20 The phase coexistence region shrinks to zero and the critical temperatures vanish as x goes to zero, as expected.

(ii) The competition between antiferromagnetism and ferromagnetism when $J_{AF} \neq 0$ leads to a discontinuous transition which prevents the formation of canted phases, as reported in Refs. 15–17. This transition also takes place at low dopings.

(iii) At moderate to high dopings, the FM-PM transition becomes discontinuous, if the AFM couplings are sufficiently large. The onset for first-order transitions at $x=1/2$ is $J_{AF}/t \approx 0.06$. Unlike the previous two cases, this transition takes place between phases of similar electronic density. First- and second-order transition lines are separated by tricritical points.

(iv) In an interval of J_{AF}/t, which depends on the doping level, we also find phase transitions between the PM and *A*-AFM and *C*-AFM phases, that are of second order (see Fig. 3). At low temperatures there appear FM, *C*-AFM, *A*-AFM, and *G*-AFM phases separated by first-order transitions with its associated phase separation regions, as shown in Fig. 1.

As we see, the DEM complemented with AFM superexchange interactions between the localized spins give rise to a very rich magnetic phase diagram that contains first- and second-order transitions between phases with different magnetic order.

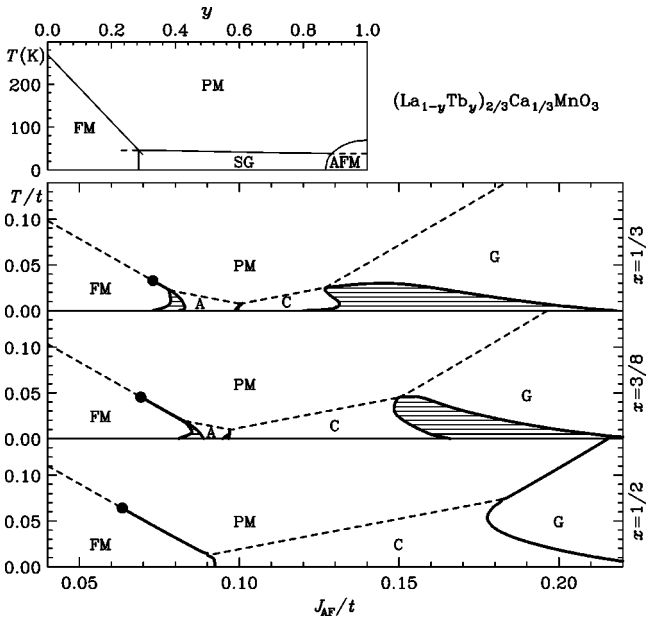

FIG. 3. Transition temperature as function of the value of J_{AF}/t for concentrations $x=1/3$, $x=3/8$, and $x=1/2$. The dashed (solid) lines correspond to continuous (first-order) transitions and a circle has been plotted at the tricritical PM-FM point. In the top panel we sketch experimental results from Ref. 46 where $x=1/3$. The compound $(La_{1-y}Pr_y)_{5/8}$ $Ca_{3/8}MnO_3$ studied in Ref. 9 has $x=3/8$.

In order to set a common frame for comparison with standard approximations,[14,20] we note the free energy of the system is made up of an entropy term, due to the thermal fluctuations of the core spins, an almost temperature-independent contribution from the electrons and another temperature-independent term due to the direct AFM coupling between the core spins. For instance, in the PM-FM case, we can write $\mathcal{F}=3J_{AF}M^2+E_{elec}(M)-TS(M)$ where $S(M)$ is the entropy of a spin in an effective magnetic field producing magnetization M. We can expand: $S(M)=-(\frac{3}{2}M^2+\frac{9}{20}M^4+\frac{99}{350}M^6+\cdots)$ and $E_{elec}(M)=c_1M^2+c_2M^4+c_3M^6+\cdots$ where c_1, c_2, and c_3 are functions of the band filling, and c_1 is always negative (c_1, c_2 and c_3 are obtained fitting the numerical results for E_{elec}). If there is a continuous transition, the critical temperature is given by $T_C=(2|c_1|-6J_{AF})/3$. The transition becomes discontinuous when the quartic term in $\mathcal{F}(M)$ is negative. This happens if $c_2<0$ and $T<20/9|c_2|$. Thus, if $J_{AF}>|c_1|/3-10|c_2|/9$ and $c_2<0$, the transition becomes of first order. A tricritical point appear in the transient between first- and second-order transitions.

The fact that $c_2<0$ is due to the energetics of the electrons in the disordered spin background. In a fully polarized system, $M=1$, the electrons propagate in a perfect lattice. If $M=0$ the spins are completely disordered, and our results reduce to those reported in Refs. 47 and 48.

Standard approximations[14,20] to the phase diagram of the DEM use the virtual crystal approximation, in which the cubic density of states is scaled by the average value $\langle \mathcal{T}(\boldsymbol{S}_i,\boldsymbol{S}_j)\rangle$, defined in Eq. (1). This approximation suffices to describe the main features of the phase diagram when

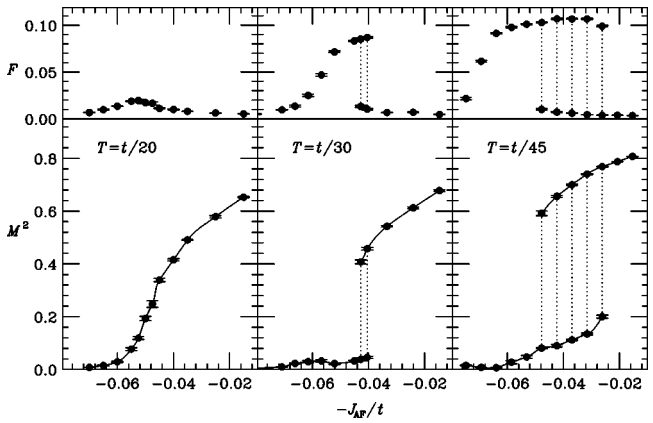

FIG. 4. Monte Carlo results for the squared magnetization (bottom), and the $\boldsymbol{k}=(2\pi/8,0,0)$ squared Fourier component of the magnetization (top) in $8\times8\times8$ lattices, as function of J_{AF}/t, for $x=1/2$ at different temperatures.

$J_{\mathrm{AF}}=0$, but overestimates the kinetic energy of the electrons moving in the disordered spin background. The effect is more pronounced near half filling, when the electronic contribution is the largest, and c_2 is positive on the virtual crystal scheme. As our calculation takes fully into account the propagation of the electrons in a disordered environment, we think that the existence of a first order PM-FM transition when T_{C} is suppressed is a robust feature of the model.

At zero temperature, our calculation leads to a richer phase diagram to that calculated within the dynamical mean-field approximation.[49] As mentioned in the preceding section, our method coincides with this approximation when implemented in a Bethe lattice. The topology of a cubic lattice allows for the possibility of *A*-AFM and *C*-AFM phases.

We have developed an exact Monte Carlo algorithm to study the DEM. This approach is based in a path-integral formulation that allows to simulate on lattices much larger than in an usual Hamiltonian formulation. Full details of the method are given in Ref. 50. The first data of the Monte Carlo computation confirm the robustness of the present results. Simulations in the parameter region depicted in Fig. 3 show indications for a strong transition in lattices up to $12\times12\times12$ sizes, between ordered and disordered phases. In Fig. 4 we show data on a $L=8$ lattice at half filling at several temperatures. It is also clear that fluctuations lower the transition temperatures from their mean-field values, as it also happens in the three-dimensional Heisenberg model.[51] In addition, we find a helicoidal spin structure at sufficiently low temperatures.

Turning again to the mean-field approach, let us recall that while a continuous transition is changed into a smooth crossover in an applied field, a first-order transition survives until a critical field is reached. The transition takes place between two phases with finite, but different, magnetization, in a similar way to the liquid-vapor transition. The PM-FM line of first-order transitions for dopings close to $x=0.5$ ends in a critical point, $(T_{\mathrm{c}},H_{\mathrm{c}})$. For $J_{\mathrm{AF}}=0.08t$, the critical field varies from $H_{\mathrm{c}}=0.000\,75t\approx2.2$ T at $x=0.5$ to $H_{\mathrm{c}}=0.0002t\approx0.6$ T at $x=0.3$, while $T_{\mathrm{c}}\approx T_{\mathrm{C}}$ and T_{C} is the Curie temperature at zero field, shown in Fig. 3.

V. CONCLUSIONS

We have shown that the phase diagram of double-exchange systems is richer than previously anticipated, and differs substantially from that of more conventional itinerant ferromagnets. We have described first-order transitions which are either intrinsic to the double-exchange mechanism, or driven by the competition between it and AFM couplings. In particular, we find that, in the doping range relevant for CMR effects, AFM interactions of reasonable magnitude change the PM-FM transition from continuous to first order. The existence of such a transition has been argued, on phenomenological grounds, in order to explain the observed data in a variety (but not all) of doped manganites in the filling range $x\sim0.3$–0.5.[52,53] The generic phase diagram that we obtain is consistent with a number of observations:

(i) Materials with a high transition temperature, like $La_{1-x}Sr_xMnO_3$ (which have small AFM couplings), have a continuous PM-FM transition, with no evidence for inhomogeneities or hysteretic effects. The paramagnetic state shows metallic behavior.

(ii) The PM-FM transition in materials with low transition temperature, like $La_{1-x}Ca_xMnO_3$, (significant AFM couplings) is discontinuous. Near T_{C} inhomogeneities and hysteretic behavior are observed. The transport properties in the paramagnetic phase are anomalous.

(iii) Substitution of a trivalent rare earth for another one with smaller ionic radius (i.e., compositional changes that do not modify the doping level) diminishes the Mn-O-Mn bond angle, reducing the conduction bandwidth, $W=12t$.[22,42,54] Assuming that the AFM coupling J_{AF} does not change significantly, the ratio J_{AF}/t increases; therefore the doping level y in series of the type $(R_{1-y}R_y)_{1-x}A_xMnO_3$ might be traded by J_{AF}/t. The top panel of Fig. 3 shows the experimental magnetic phase diagram of $(La_{1-y}\ Tb_y)_{2/3}\ Ca_{1/3}MnO_3$, as taken from Ref. 46. We note the similarities with the phase diagrams of the DEM in the plane $(J_{\mathrm{AF}}/t,T/t)$ at fixed x. The phases *A*-AFM and *C*-AFM at intermediate J_{AF}/t could become spin-glass-like phases in presence of disorder.

(iv) The first-order PM-FM transition reported here survives in the presence of an applied field. A critical field is required to suppress it (hysteretic effects in an applied field have been reported in Ref. 55).

Note that the relevance of the ratio J_{AF}/t in explaining the different behavior of compounds with the same nominal doping was already emphasized, on phenomenological grounds, in Refs. 21 and 22.

ACKNOWLEDGMENTS

We are thankful for helpful conversations to L. Brey, J. Fontcuberta, G. Gómez-Santos, C. Simon, J. M. De Teresa, and especially to R. Ibarra. V.M.-M. acknowledges the financial support of MEC. The Monte Carlo simulations have been carried out in RTNN computers at Zaragoza and Madrid. We acknowledge financial support from Grant Nos. PB96-0875, AEN97-1680, AEN97-1693, AEN99-0990 (MEC, Spain), and (07N/0045/98) (C. Madrid).

[1] E. D. Wollan and W. C. Koehler, Phys. Rev. **100**, 545 (1955).
[2] D. I. Khomskii and G. Sawatzky, Solid State Commun. **102**, 87 (1997).
[3] J. M. D. Coey, M. Viret, and S. von Molnar, Adv. Phys. **48**, 167 (1999).
[4] C. Zener, Phys. Rev. **82**, 403 (1951).
[5] P. W. Anderson and H. Hasegawa, Phys. Rev. **100**, 675 (1955).
[6] A. J. Millis, P. B. Littlewood, and B. I. Shraiman, Phys. Rev. Lett. **74**, 5144 (1995).
[7] J. van den Brink, G. Khaliullin, and D. Khomskii, Phys. Rev. Lett. **83**, 5118 (1999); T. Mizokawa, D. I. Khomskii, and G. A. Sawatzky, Phys. Rev. B **61**, R3776 (2000).
[8] J. de Teresa, M. R. Ibarra, P. A. Algarabel, C. Ritter, C. Marquina, J. Blasco, J. García, A. del Moral, and Z. Arnold, Nature (London) **386**, 256 (1997).
[9] M. Uehara, S. Mori, C. H. Chen, and S.-W. Cheong, Nature (London) **399**, 560 (1999).
[10] M. Fäth, S. Freisem, A. A. Menovsky, Y. Tomioka, J. Aarts, and J. A. Mydosh, Science **285**, 1540 (1999).
[11] J. Fontcuberta, B. Martínez, A. Seffar, S. Piñol, J. L. García-Muñoz, and X. Obradors, Phys. Rev. Lett. **76**, 1122 (1996).
[12] J. A. Fernández-Baca, P. Dai, H. Y. Hwang, C. Kloc, and S.-W. Cheong, Phys. Rev. Lett. **80**, 4012 (1998).
[13] J. Mira, J. Rivas, F. Rivadulla, C. Vázquez-Vázquez, and M. A. López-Quintela, Phys. Rev. B **60**, 2998 (1999).
[14] P.-G. de Gennes, Phys. Rev. **118**, 141 (1960).
[15] E. L. Nagaev, Physica B **230-232**, 816 (1997).
[16] J. Riera, K. Hallberg, and E. Dagotto, Phys. Rev. Lett. **79**, 713 (1997).
[17] D. P. Arovas and F. Guinea, Phys. Rev. B **58**, 9150 (1998).
[18] In the De Gennes study of this model (Ref. 14), the coupling constant was chosen ferromagnetic between spins lying on the same $z=$ const plane, and antiferromagnetic between spins siting on neighboring planes. This is a reasonable starting point for the study of $La_{1-x}Ca_xMnO_3$ if $x<0.16$ where *A*-type antiferromagnetism is found. For larger doping, $0.16<x<0.5$, which is our main focus, magnetism is uniform and there is no *a priori* reason for privileging a particular direction. We shall show however that even within our isotropic model *A*-type antiferromagnetism can appear if the competition between the double-exchange mechanism and the antiferromagnetic coupling is strong enough.
[19] S. Yunoki, J. Hu, A. L. Malvezzi, A. Moreo, N. Furukawa, and E. Dagotto, Phys. Rev. Lett. **80**, 845 (1998).
[20] D. Arovas, G. Gómez-Santos, and F. Guinea, Phys. Rev. B **59**, 13 569 (1999).
[21] H. Y. Hwang, S-W. Cheong, P. G. Radaelli, M. Marezio, and B. Batlogg, Phys. Rev. Lett. **75**, 914 (1995).
[22] J. L. García-Muñoz, J. Fontcuberta, B. Martínez, A. Seffar, S. Piñol, and X. Obradors, Phys. Rev. B **55**, R668 (1997).
[23] T. Hotta, Y. Takada, H. Koizumi, and E. Dagotto, Phys. Rev. Lett. **84**, 2477 (2000).
[24] D. Khomskii, cond-mat/0004034 (unpublished).
[25] R. H. Heffner, D. E. MacLaughlin, G. J. Nieuwenhuys, T. Kimura, G. M. Luke, Y. Tokura, and Y. J. Uemura, Phys. Rev. Lett. **81**, 1706 (1998).
[26] M. Medarde, J. F. Mitchell, J. E. Millburn, S. Short, and J. D. Jorgensen, Phys. Rev. Lett. **83**, 1223 (1999).
[27] L. Vasiliu-Doloc, S. Rosenkranz, R. Osborn, S. K. Sinha, J. W. Lynn, J. Mesot, O. H. Seeck, G. Preosti, A. J. Fedro, and J. F. Mitchell, Phys. Rev. Lett. **83**, 4393 (1999).
[28] B. García-Landa, C. Marquina, M. R. Ibarra, G. Balekrishnan, M. R. Lees, and D. McK. Paul, Phys. Rev. Lett. **84**, 995 (2000).
[29] M. R. Ibarra, P. A. Algarabel, C. Marquina, J. Blasco, and J. García, Phys. Rev. Lett. **75**, 3541 (1995).
[30] C. H. Booth, F. Bridges, G. H. Kwei, J. M. Lawrence, A. L. Cornelius, and J. J. Neumeier, Phys. Rev. Lett. **80**, 853 (1998).
[31] J. L. Alonso, L. A. Fernández, F. Guinea, V. Laliena, and V. Martín-Mayor, cond-mat/0007438 Phys. Rev. B (to be published).
[32] See, e.g., G. Parisi, *Statistical Field Theory* (Addison Wesley, New York, 1988).
[33] C. Benoit, E. Royer, and G. Poussigue, J. Phys.: Condens. Matter **4**, 3125 (1992), and references therein; C. Benoit, *ibid.* **1**, 335 (1989); G. Viliani, R. Dell'Anna, O. Pilla, M. Montagna, G. Ruocco, G. Signorelli, and V. Mazzacurati, Phys. Rev. B **52**, 3346 (1995); V. Martín-Mayor, G. Parisi, and P. Verrocchio, Phys. Rev. E **62**, 2373 (2000).
[34] P. Turchi, F. Ducastelle, and G. Treglia, J. Phys. C **15**, 2891 (1982).
[35] N. Furukawa, cond-mat/9812066 (unpublished).
[36] A. Georges, G. Kotliar, W. Krauth, and M. J. Rozenberg, Rev. Mod. Phys. **68**, 13 (1996).
[37] F. Guinea, G. Gómez-Santos, and D. P. Arovas, Phys. Rev. B **62**, 391 (2000)
[38] G. Gómez-Santos (private communication).
[39] Whether the presence of nonsaturated AFM phases is an artifact of our mean-field *Ansätze* of a real feature of the model is a rather difficult question to answer. The following heuristic argument suggest that close to half filling, it might be true. Let us consider the following spin configurations: in all the *even* sites (as given by the parity of $x+y+z$) we put the spins along the positive *z* axis, while in the odd sites, we put the spins randomly on a cone making an angle α with the negative *z* axis. The density of states is the one of a perfect crystal with hopping integral $t\sin\alpha/2$, while the exchange energy per spin is $-3J_{AF}\cos\alpha$. It is clear that the perfect antiferromagnetic configuration is not the true energy minimum of the system, that instead is found at a value of α of order t/J_{AF}. The situation is perfectly analogous to an antiferromagnetic Potts model on the cubic lattice, with more than two states (see, for instance, Ref. 39): a large set of degenerated ground states of the system (but not all!) have the spins of the even sublattice on (say) the 0 state and the spins on the odd sublattice randomly on all the available states different from 0. In Ref. 40 it has been proved that if the number of available states is larger than twice the coordination number of the lattice, the Potts model has a finite entropy even at zero temperature. Since the number of available states for us is infinite (we can put the spins wherever we like on a cone), one is tempted to conclude that nonsaturated phases are indeed found even at zero temperature.
[40] J. Salas and A. Sokal, J. Stat. Phys. **86**, 551 (1997).
[41] W. E. Pickett and D. J. Singh, Phys. Rev. B **53**, 1146 (1996).
[42] J. L. García-Muñoz, J. Fontcuberta, M. Suaaid, and X. Obradors, J. Phys.: Condens. Matter **8**, L787 (1996).
[43] V. Laukhin, J. Fontcuberta, J. L. García-Muñoz, and X. Obradors, Phys. Rev. B **56**, R10009 (1997).
[44] F. Moussa, M. Hennion, J. Rodríguez-Carvajal, H. Moudden, L. Pinsard, and A. Revcolevschi, Phys. Rev. B **54**, 15 149 (1996);

M. Hennion, F. Moussa, J. Rodríguez-Carvajal, L. Pinsard, and A. Revcolevschi, *ibid.* **56**, R497 (1997).

[45] I. Panas, R. Glatt, and T. Johnson, J. Phys. Chem. Solids **59**, 2230 (1998).

[46] J. M. De Teresa, C. Ritter, M. R. Ibarra, P. A. Algarabel, J. L. García-Muñoz, J. Blasco, J. García, and C. Marquina, Phys. Rev. B **56**, 3317 (1997).

[47] J. Zang, A. R. Bishop, and H. Röder, Phys. Rev. B **53**, R8840 (1996); Q. Li, J. Zang, A. R. Bishop, and C. M. Soukoulis, *ibid.* **56**, 4541 (1997).

[48] M. J. Calderón, J. A. Vergés, and L. Brey, Phys. Rev. B **59**, 4170 (1999).

[49] A. Chattopadhyay, A. J. Millis, and S. Das Sarma, cond-mat/0004151 (unpublished).

[50] J. L. Alonso, L. A. Fernández, F. Guinea, V. Laliena, and V. Martín-Mayor, cond-mat/0007450, Nucl. Phys. B (to be published).

[51] H. G. Ballesteros, L. A. Fernández, V. Martín-Mayor, and A. Muñoz-Sudupe, Phys. Lett. B **387**, 125 (1996).

[52] R. H. Heffner, J. E. Sonier, D. E. MacLaughlin, G. J. Nieuwenhuys, G. Ehelers, F. Mezei, S.-W. Cheong, J. S. Gardner, and H. Roder, cond-mat/9910064 (unpublished); V. Podzorov, M. Uehara, M. E. Gershenson, T. Y. Koo, and S.-W. Cheong, Phys. Rev. B **61**, R3784 (2000).

[53] A. Moreo, M. Mayr, A. Feiguin, S. Yunoki, and E. Dagotto, Phys. Rev. Lett. **84**, 5568 (2000).

[54] J. Fontcuberta, V. Laukhin, and X. Obradors, Phys. Rev. B **60**, 6266 (1999).

[55] R. P. Borges, F. Ott, R. M. Thomas, V. Skumryev, J. M. D. Coey, J. I. Arnaudas, and L. Ranno, Phys. Rev. B **60**, 12 847 (1999).